

Omnidirectional resonance in a metal–dielectric–metal geometry

Hocheol Shin, Mehmet Fatih Yanik, and Shanhui Fan^{a)}

Department of Electrical Engineering, Stanford University, Stanford, California 94305

Rashid Zia and Mark L. Brongersma

Department of Material Science and Engineering, Stanford University, Stanford, California 94305

(Received 22 December 2003; accepted 6 April 2004; published online 12 May 2004)

We show that a planar metallic microcavity structure can exhibit an omnidirectional resonance, i.e., a resonance for which the resonance wavelength is independent of the incidence angle of light. The structure consists of a metal–dielectric–metal configuration. The omnidirectional resonance occurs when the reflection phase shift cancels the propagation shift. We numerically demonstrate such an omnidirectional resonance in an Ag–SiO₂–Ag structure with realistic material parameters. Such omnidirectionally resonant structures are important for all-angle efficiency enhancement in light emitting diodes and photodetectors. © 2004 American Institute of Physics.

[DOI: 10.1063/1.1758306]

Planar microcavity structures have been widely used to provide resonant enhancement of performance in optoelectronic devices such as light emitting diodes,¹ photodetectors,² modulators,³ and amplifiers.⁴ In all previous works, resonant enhancement at a given wavelength occurs only within a very narrow angular range. Such effect has limited the applications of planar microcavity structures where a wide angular range of input or output is required.⁵

In this letter, we introduce a microcavity structure in which the resonance wavelength is independent of angle of incidence (we refer to such a resonance as an omnidirectional resonance). The structure consists of a metal–dielectric–metal (MDM) configuration, as shown in the inset of Fig. 1(a), and operates at the surface plasmon frequency (ω_{sp}) of the metal–dielectric interface. We further provide a realistic design, using documented material parameters and illustrate the effects of material losses.

The operating principle of the omnidirectional resonance can be best understood by considering the dispersion relation for a MDM structure [Fig. 1(a)], in which both metal regions are semi-infinite.⁶ As a starting point, we use the lossless Drude model for the metal dielectric function:

$$\epsilon(\omega) = 1 - \frac{\omega_p^2}{\omega^2}, \quad (1)$$

where ω_p is the plasma frequency, and calculate the dispersion relation with transfer matrix formalism.⁷ The dispersion relation relates the frequency ω and the wave vector k_{\parallel} parallel to the interface for all the eigenmodes. The modes that are confined in the dielectric region exhibit three discrete bands labeled as I, II, III, respectively. All these modes have TM polarization with magnetic field perpendicular to the wave propagation direction.

The modes in band II are of particular interest because a significant portion of their dispersion relation lies above the light line of air. Consequently, externally incident light can couple to this band when one of the metal regions is of finite

thickness.⁸ When k_{\parallel} approaches infinity, $\omega_{II}(k_{\parallel})$ (i.e., the dispersion frequency of band II as a function of k_{\parallel}) approaches ω_{sp} . At this frequency, the metal dielectric constant (ϵ_{metal}) is equal in magnitude and opposite in sign to that of the dielectric ($\epsilon_{\text{dielectric}}$):⁹

$$\epsilon_{\text{dielectric}} = -\epsilon_{\text{metal}}. \quad (2)$$

At $k_{\parallel}=0$, $\omega_{II}(k_{\parallel}=0)$ varies with the thickness d of the dielectric region, and coincides with ω_{sp} when

$$d = \frac{\lambda_{sp}}{4\sqrt{\epsilon_{\text{dielectric}}}}, \quad (3)$$

where λ_{sp} is the free-space surface plasmon wavelength ($=2\pi c/\omega_{sp}$). In this case, a full calculation shows that band II becomes almost completely flat [Fig. 1(a)]. For incident light at a given wavelength, the wave vector k_{\parallel} is determined by the incidence angle. Such a flat dispersion band, therefore, indicates that the resonance occurs approximately at the same wavelength for all incidence angles.

A vector plot of the electric field for a mode in band II is shown in Fig. 1(b). The field distribution is symmetric about the center plane of the structure. All the electric field lines originate and terminate at the same metal–dielectric interface. At the center of the dielectric region, the field lines are parallel to the interfaces. Therefore, such a mode should strongly couple to a dipole moment placed parallel to the interfaces at the center of the dielectric region, resulting in an all-angle resonant enhancement of radiation from the dipole moment at a given frequency.

The physical reason of an omnidirectional resonance can be illustrated by considering the phase of the reflected wave at the metal–dielectric interface. For a TM wave at a frequency where Eq. (2) is satisfied, the reflection coefficient for the magnetic field at the interface is⁷

$$\Gamma = \frac{\cos\theta - i\sqrt{1 + \sin^2\theta}}{\cos\theta + i\sqrt{1 + \sin^2\theta}}, \quad (4)$$

where θ is the incidence angle. The magnitude of the reflection coefficient is unity at all angles while the phase varies

^{a)}Electronic mail: shanhui@stanford.edu

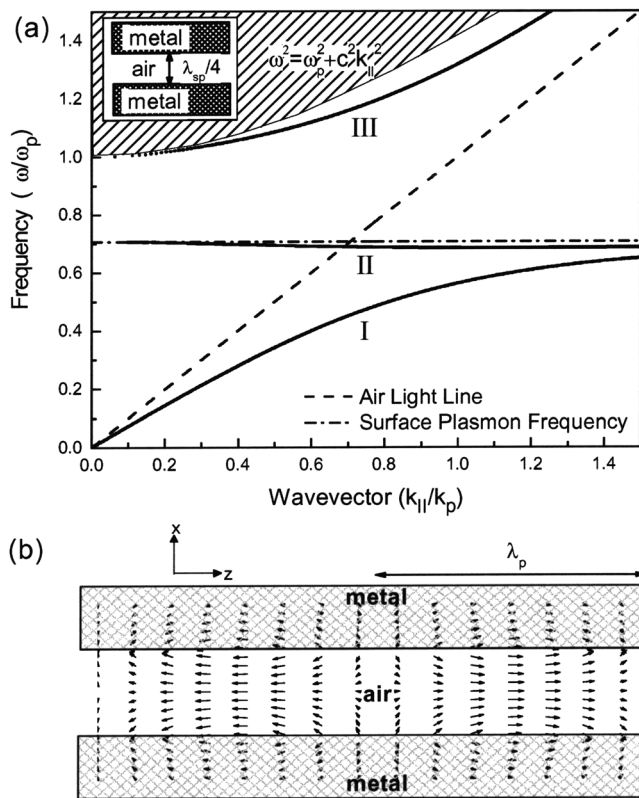


FIG. 1. (a) Dispersion relation of a MDM structure in which the dielectric region is air ($\epsilon_r = 1$) and is $\lambda_{sp}/4$ thick. The structure is shown in the inset. The frequency and the wave vector are normalized with respect to ω_p and k_p where $k_p = \omega_p/c$; c is the speed of light in free space. The solid lines labeled by I, II, III represent the modes that are confined in the dielectric region. The modes in bands I and III have odd electric field distribution while the modes in band II have even electric field distribution with respect to the center plane of the structure. The shaded area represents the continuum of modes that are extended in metals. (b) Vector plot of the electric field of a mode in band II at $k = 0.48k_p$. λ_p is the plasma wavelength ($= 2\pi c/\omega_p$).

with θ . At normal incidence, the reflected wave acquires 90° phase shift. The phase shift increases with θ , reaching 180° at the grazing incidence. When the dielectric thickness satisfies Eq. (3) in the MDM structure, the aggregate reflection phase shift at the metal–dielectric interfaces almost exactly cancels the phase shift due to the propagation of the wave in the direction perpendicular to the interfaces in the dielectric region, leading to an approximate 2π shift on each round trip for all θ 's (Fig. 2).

Based on the discussions above, the omnidirectional resonance should occur as long as both Eqs. (2) and (3) are satisfied. Therefore, such a resonance can be observed in realistic material systems, and is in fact not limited to an idealized metal described by the Drude model. In the presence of material loss, our numerical simulations show that Eqs. (2) and (3) still represent approximate conditions for an omnidirectional resonance, provided that we use the real part of metal dielectric function in Eq. (2).

We demonstrate the omnidirectional resonance in a realistic system in the presence of material loss using documented material properties for Ag and SiO_2 .¹⁰ The frequency response of the system is calculated with the transfer matrix formalism. The effect of the omnidirectional resonance can be probed by coupling incident light to the micro-

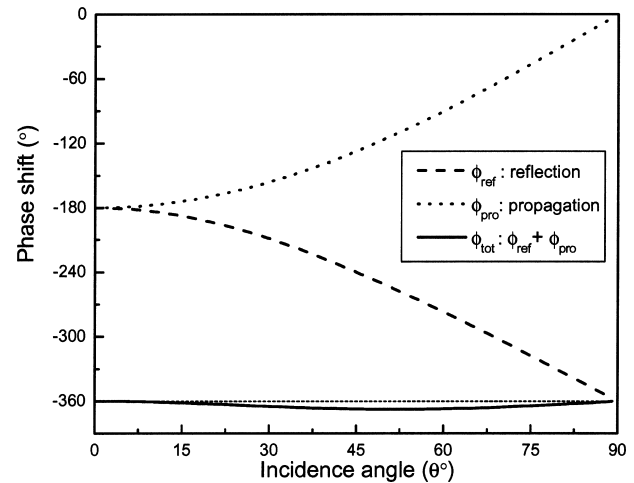


FIG. 2. The round-trip phase shift in the MDM structure shown in Fig. 1(a) at ω_{sp} as a function of incidence angle. The dashed line shows the aggregate reflection phase shift at the two interfaces and the dotted line shows the propagation phase shift in the surface normal in the dielectric. The total round-trip phase shift represented by the solid line is approximately 360° , satisfying the resonance condition at every incidence angle.

cavity through the top metal layer (Fig. 3, inset). Consequently, the top layer needs to be thin enough to allow light to pass through. At the same time, the top layer still needs to retain sufficient thickness such that the phase shift upon reflection can still be approximated by Eq. (4), and that the dispersion relation of the cavity deviates little from an ideal structure that has semi-infinite Ag regions. Empirically, we find that the top Ag layer with a thickness of 38 nm satisfies both requirements. Also, we find that the optimal thickness of the SiO_2 region is 56 nm, which is close to the prediction of Eq. (3). To demonstrate the omnidirectional resonance, we vary the angle of incidence and calculate the electromagnetic energy inside the cavity as plotted in Fig. 3. For every angle, the energy peaks around the same wavelength of 352 nm, which is very close to the prediction of Eq. (2). The resonance energy in the cavity decreases at large incidence angles due to material loss. Nevertheless, the resonance still

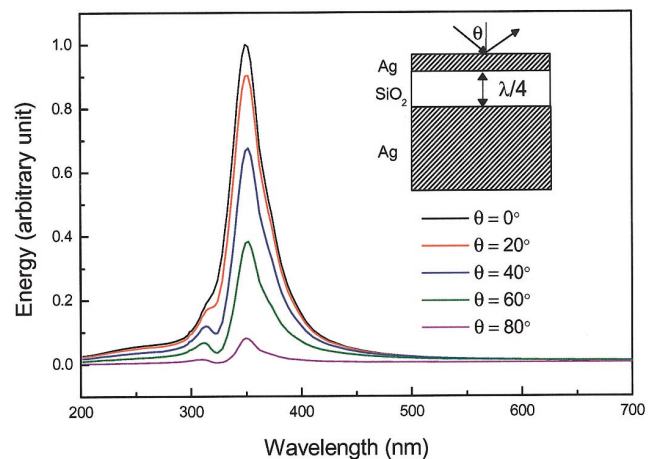


FIG. 3. (Color) Total electromagnetic energy in the dielectric region of the structure as a function of wavelength of incident light for incidence angles ranging from 0° to 80° . The incident electromagnetic flux for all angles is the same. The schematic of the microcavity structure is shown in the inset. The top Ag film and the SiO_2 region are 38- and 56-nm-thick, respectively. The energy peaks around 352 nm for each incidence angle.

persists even at a large angle of 80° . At the center of the cavity, such a resonance has its electric field parallel to the interfaces. The cavity structure would, therefore, provide omnidirectional resonant enhancement of either emission or absorption for a dipole inside the cavity that is directed parallel to the interfaces. Also, the resonance can be designed to occur at other wavelengths by appropriate selection of metal and dielectric combination that satisfies Eq. (2). Experimentally, this resonance can also be probed by measuring the reflection spectrum of the cavity at various incidence angles. The resonance appears as an angular-independent dip in the reflection spectrum.

This work is supported in part by NSF Grant Nos. ECS-0134607 and CCR-0303884. The authors also acknowledge

the support of Samsung Lee Kun Hee fellowship (H.S.), and Stanford graduate fellowships (R.Z. and M.F.Y.).

¹E. F. Schubert, N. E. Hunt, M. Micovic, R. J. Malik, D. L. Sivco, A. Y. Cho, and G. J. Zydzik, *Science* **265**, 943 (1994).

²A. Chin and T. Y. Chang, *J. Lightwave Technol.* **9**, 321 (1991).

³R. J. Simes, R. H. Yan, R. S. Geels, L. A. Coldren, J. H. English, A. C. Gossard, and D. G. Lishan, *Appl. Phys. Lett.* **53**, 637 (1988).

⁴M. Lipson and L. C. Kimerling, *Appl. Phys. Lett.* **77**, 1150 (2000).

⁵M. S. Unlu and S. Strite, *J. Appl. Phys.* **78**, 607 (1995).

⁶E. N. Economou, *Phys. Rev.* **182**, 539 (1969).

⁷M. Born and E. Wolf, *Principles of Optics*, 6th ed. (Cambridge University Press, Cambridge, 1980).

⁸F. Villa, T. Lopez-Rios, and L. E. Regalado, *Phys. Rev. B* **63**, 165103 (2001).

⁹H. Raether, *Surface Plasmons on Smooth and Rough Surfaces and on Grating* (Springer, Berlin, 1988).

¹⁰E. D. Palik, *Handbook of Optical Constants of Solids* (Academic, San Diego, 1985).